

New data on the crystal-chemistry of fluoborite by means of SREF, SIMS, and EMP analysis

Fernando Cámara* and Luisa Ottolini

CNR-Centro di Studio per la Cristallografia e la Cristallografia, via Ferrata 1, I-27100 Pavia, Italy

ABSTRACT

The crystal structure of fluoborite [$\text{Mg}_3\text{F}_3(\text{BO}_3)$] was refined by Dal Negro and Tadini (1974) who provided a complete structural model. Previously, Takeuchi (1950) had refined an OH-dominant fluoborite (OH ~70%), but the limited quantity of data (extracted from two Weissenberg-Buerger photographs) did not permit the location of H atoms. Dal Negro and Tadini (1974) also could not locate H atoms because they used a crystal with near end-member composition. We have located the H bond in an OH-dominant fluoborite from the Betic Cordilleras (SE Spain). Excellent quality X-ray data on two crystals of fluoborite allowed discovery and refinement of the H position in this mineral. Electron microprobe (EMP) and secondary-ion mass spectrometry (SIMS) analyses of the light elements H, B, and F have resulted in the formulation of special procedures to obtain accurate, high-quality quantitative data, which are presented in this paper. EMP, SIMS, and crystal structure refinement (SREF) data are in a good agreement. Linear equations are also presented to calculate the F content directly from cell parameters.

INTRODUCTION

Fluoborite is a rare mineral found in contact metamorphosed marble. It was first described by Geijer (1926) from Norberg (Sweden), where it was associated with norbergite. Following the proposal of Hawthorne (1983) for classification of borate-group minerals, which is based on the polymerization of high bond-valence polyhedra (in borates, the BO_3 and BO_4 polyhedra) or fundamental building blocks (FBB; Hawthorne et al. 1996), fluoborite is classified as the simplest borate and consists of homopolyhedral clusters of triangular-coordination BO_3 polyhedra. It belongs to the 3 Å wallpaper structures group of Moore and Araki (1974) and contains pairs of edge-sharing infinite octahedral chains, forming ribbons along [001], cross-linked by BO_3 triangles. These octahedral chains repeat every 3 Å along their length. The ribbons share vertices forming triangular and hexagonal tunnels. The triangular tunnels are filled with boron in triangular coordination with oxygen, and perpendicular to the *c* axis, whereas the hexagonal tunnels are empty.

The structure of fluoborite was determined by Takeuchi (1950), who described it as hexagonal with space group $C6_3/m$. The structure was confirmed by Dal Negro and Tadini (1974) who also confirmed the centrosymmetric character of this structure and proposed $P6_3/m$ as the space group. Natural fluoborite exhibits complete $\text{OH}^- \rightarrow \text{F}^-$ substitution. In the past, the F-end-member was called “nocerite” (Brisi and Eitel 1957). The samples studied here represent a F-rich fluoborite in which the *a* unit-cell parameter (= 8.861 Å) falls between the values reported

by Takeuchi (1950) and by Dal Negro and Tadini (1974) (= 9.06 and 8.827 Å, respectively), indicating a high F content and the presence of some OH.

EXPERIMENTAL PROCEDURES AND RESULTS

Sample description

Fluoborite crystals were hand-picked from a crushed sample of metamorphosed and metasomatized marble (HV-43) from Huerta del Vinagre, a small scheelite mine that crops out in the Guadaiza Unit of the Upper Alpujarride series, in the Betic Cordilleras, Spain. This sample is a magnesian skarn formed by interaction between dolomitic marbles and magmatic fluids from the surrounding granites. In particular, the sample represents an exoskarn almost entirely composed of monomineralic, metasomatic veins of calcite and humite-group minerals, with rare fluoborite and minor serpentine (from alteration of humite-group minerals). The humite-group minerals in these samples have very low Fe and Ti contents (Cámara 1997; Ottolini et al. 2000).

Single-crystal structure refinement

Data collection and refinement were carried out for crystals Fbor HV-43 n.2 and Fbor HV-43 n.3 with an automatic 4-circle Philips PW1100 diffractometer, using graphite-monochromatized MoK α radiation. The space group $P6_3/m$ has been confirmed. Unit-cell parameters [*a* = 8.8612(12) Å, *c* = 3.1021(6) Å for Fbor HV-43 n.2; *a* = 8.8602(12) Å, *c* = 3.1021(6) Å for Fbor HV-43 n.3] were calculated from a least-squares refinement of *d* calculated for 56 rows of the reciprocal lattice by measuring the reflections in the range $-35^\circ < \theta < 35^\circ$. They are reported in Table 1 together with R-factors. Three equivalent hexagonal reflections (*hkl*, $\bar{h}kl$, and $h\bar{k}l$) were collected in the θ range 2–35°. The profiles were integrated following the method of Lehmann and Larsen (1974)

*Present address: Laboratoire Structure et Propriétés Etat Solide, Université Sciences et Technologies de Lille, Bat C6, 59655 Villeneuve d'Ascq-Cedex, France.
E-mail: fernando.camara@univ-lille1.fr

TABLE 1. Unit-cell parameters and selected SREF results

	Fbor HV-43 n.2	Fbor HV-43 n.3
code	fwf	gal
a (Å)	8.8612(12)	8.8602(12)
c (Å)	3.1021(6)	3.1021(6)
V (Å ³)	210.95	210.95
Z	3	3
θ range (°)	2–35	2–35
Rsym*	3.4	1.6
no. ref. per.	26	26
R _w †	1.95(353)	2.09(346)
GoF‡	0.9931	1.0085
R _{int}	1.28(336)	1.33(328)

Note: Code = symbolic address in the CSCC data base.

* Merging agreement factor.

† Weighted refinement agreement factor and number of reflections between parentheses.

‡ Goodness of Fit.

isotropic atomic displacement parameters (a.d.p.) are reported in Table 2a, anisotropic a.d.p. in Table 2b, selected geometrical parameters in Table 3, and observed and calculated structure factors in Tables 4a and 4b.¹

EMP analyses

The crystals were mounted in epoxy resin and polished. Sample Fbor HV-43 n.2 was embedded with its *c* axis parallel to the polishing surface (i.e., perpendicular to the electron beam), and Fbor HV-43 n.3 with its *c* axis perpendicular to the polishing surface. Both were analyzed with an ARL-SEMQ electron microprobe equipped with four spectrometers (RAP, PET, LiF200, and ADP crystals) at the Dipartimento di Scienze della Terra, University of Modena (Italy). Natural minerals were used as standards. A fluorite from Carrara Marbles was used as

TABLE 2a. Site scattering, fractional atomic coordinates and isotropic atomic displacement parameters

	Atom	s.s.*	X/A	Y/B	Z/C	B _{eq}
Fbor HV-43 n.2	O	8.00	0.55223 (7)	0.15481 (7)	3/4	0.49 (1)
Fbor HV-43 n.3	O	8.00	0.55233 (7)	0.15487 (7)	3/4	0.50 (1)
	F	8.80	0.29653 (8)	0.20836 (7)	1/4	0.80 (2)
	F	8.80	0.29646 (8)	0.20828 (7)	1/4	0.81 (2)
	B	4.89	2/3	1/3	3/4	0.35 (2)
	B	4.86	2/3	1/3	3/4	0.36 (2)
	Mg	12.11	0.36904 (4)	0.03123 (4)	1/4	0.51 (1)
	Mg	12.03	0.36902 (4)	0.03119 (4)	1/4	0.50 (1)
	H	0.19	0.168	0.113	1/4	1.02
	H	0.23	0.167	0.111	1/4	4.34

* s.s. = site scattering in electrons.

TABLE 2b. Anisotropic atomic displacement parameters

		B ₁₁	B ₂₂	B ₃₃	B ₁₂	B ₁₃	B ₂₃
Fbor HV-43 n.2	O	0.00201 (6)	0.00152 (7)	0.01510 (48)	0.00070 (6)	0	0
Fbor HV-43 n.3	O	0.00205 (6)	0.00161 (7)	0.01477 (49)	0.00069 (6)	0	0
	F	0.00545 (8)	0.00333 (8)	0.01555 (50)	0.00302 (6)	0	0
	F	0.00555 (9)	0.00337 (8)	0.01582 (52)	0.00307 (6)	0	0
	B	0.00158 (15)	0.00158	0.00759 (129)	0.00079	0	0
	B	0.00155 (16)	0.00155	0.00930 (134)	0.00077	0	0
	Mg	0.00247 (5)	0.00211 (5)	0.01244 (34)	0.00122 (3)	0	0
	Mg	0.00241 (6)	0.00211 (5)	0.01245 (36)	0.00122 (4)	0	0

as modified by Blessing et al. (1974). Intensities were corrected for Lorentz-polarization and absorption following North et al. (1968), and the equivalent pairs were merged giving $R_{\text{sym}} = 3.4\%$ and 1.6% .

Weighted, full-matrix least-square refinements were carried out using a modified version of ORFLS (Busing et al. 1962). Scattering factors were taken from the International Tables for Crystallography: neutral vs. ionized scattering-factors were used for the O site (Ungaretti et al. 1983); vacancy vs. neutral B in the B site; F⁻ vs. O⁻ for the F site; vacancy vs. H⁺ in the H site; and Mg²⁺ vs. Fe²⁺ in the Mg octahedral sites.

In the refined crystal, a Fourier-difference map showed some residual maxima at convergence. The most important maximum (peak height of $0.46 \text{ e}^{-}/\text{Å}^3$) was identified as bonding electrons in the middle of the B-O bond (0.67 Å from B); another maximum at 1.08 Å from F, with a peak height of $0.35 \text{ e}^{-}/\text{Å}^3$, was refined as a probable H atom due to its position (even if its electronic density was rather low) allowing a significant decrease of the R^2 factors and of the estimated standard deviations (e.s.d.) of the refined parameters. No other peak position with peak height greater than $0.28 \text{ e}^{-}/\text{Å}^3$ was observed.

Fractional coordinates, refined site scattering (s.s.), and

TABLE 3. Selected geometrical parameters

		Fbor HV-43 n.2	Fbor HV-43 n.3
B-O	×3	1.3880 (6)	1.3873 (6)
Mg-O	×2	2.1124 (5)	2.1129 (5)
Mg-O		2.0867 (7)	2.0862 (7)
Mg-F		1.9711 (6)	1.9707 (7)
Mg-F	×2	2.0115 (4)	2.0115 (5)
mean		2.0509	2.0510
V (Å ³)		11.365	11.367
OQE*		1.0088	1.0087
OAV*		28.31	28.19
H-H		2.0332 (3)	2.0266 (2)
(EO)-H		1.0241 (6)	1.0344 (6)

Note: distances in Å; OQE = octahedral quadratic elongation OAV = octahedral angle variance.

* Following Robinson et al. (1971).

¹For a copy of Table 4, document item AM-00-031, contact the Business Office of the Mineralogical Society of America (see inside front cover of recent issue) for price information. Deposit items may also be available on the American Mineralogist web site (<http://www.minsocam.org> or current web address).

the standard for F. An accelerating voltage of 15 kV and a beam current of 20 nA were used during analysis. Counting times were 20 seconds, with a spot size of 30 μm . The $\phi(\rho z)$ correction was applied (Armstrong 1988). Fluorine was analyzed with a RAP crystal. The $FK\alpha$ peak position was located on the fluoborite crystal before its analysis. Analyzing F in fluoborite at the $FK\alpha$ peak position from fluorite yields fluorine contents 7% lower than those obtained by centering on the peak from the fluoborite crystal. Area peak factors (APFs) were calculated and applied (Ottolini et al. 2000).

The chemistry of this sample is quite simple, involving only Mg, B, and F (Fe and H in minor quantities), with Mg being the main constituent (~64 wt% MgO). The average of analyses and normalized structural formulae are reported in Table 7 of Ottolini et al. (2000, this issue).

Secondary Ion Mass Spectrometry

SIMS investigations were carried out using a Cameca IMS 4f ion microprobe installed at C.N.R.-CSCC, Pavia. A $^{16}\text{O}^-$ primary ion beam with 2–5 nA current intensity was used. ^1H , ^{11}B , ^{19}F , ^{24}Mg , ^{25}Mg , and ^{30}Si isotopes were monitored as secondary positive ions with medium-high emission kinetic energies in the range ~75–125 eV. Due to the high content of fluorine, light-element determination required highly accurate characterization of chemical-matrix effects. This was achieved by choosing samples with chemical composition similar to fluoborite as standards (Ottolini et al. 2000). We present here for the first time accurate H and B analyses in fluoborite and discuss their agreement with SREF data.

Fluorine. We followed an empirical approach, using a calibration curve to quantify fluorine, with Mg selected as the matrix-reference element and F concentrations measured by EMPA. Several crystals of humite-group minerals were used as reference materials (Ottolini et al. 2000). In order of increasing F content they are clinohumite (Chum HV-41 n.3 and n.2), chondrodite (Chond HV-43 n.3 and n.4), and norbergite (Norb HV-47 n.7, Norb HV-43 n.4 and Norb HV-47 n.1). A perfectly linear working curve [regression coefficient: $R^2 = 0.97$; ion intensity ratio F^+/Mg^+ vs. $F(\text{at})/Mg(\text{at})$, where (at) represents the percentage of atomic concentration] was obtained for all

the samples (Fig. 2b in Ottolini et al. 2000). The ion yield for F relative to Mg [defined as: $IY(F/Mg) = F^+/Mg^+/F(\text{at})/Mg(\text{at})$] in fluoborite for both orientations is lower than the slope of the working curve by $\leq 8\%$. In Table 5, which compares analysis data obtained by SIMS and SREF, we note a major discrepancy in F content (~17% relative) for Fbor HV-43 n.2, against ~11% relative for Fbor HV-43 n.3. Such a discrepancy is higher than that existing between SREF and EMPA data, even considering the entire set of calibration samples. We ascribe this difference to the existence of SIMS matrix effects in F- (and B-) enriched samples. Furthermore, in the mutual comparison of the two fluoborite crystals (Table 5), the discrepancy between the two crystallographic orientations (~7% rel.) is comparable to the uncertainty of analysis (2σ).

Boron. To quantify boron accurately, a different strategy was followed due to the lack of a primary Mg-rich, B reference sample. The boron-silicate standard glass Pyrex (80.61 wt% SiO_2 , 12.86 wt% B_2O_3 , and 4.24 wt% Na_2O) and the international glass NIST-610 (72 wt% SiO_2 , and 0.113 wt% B_2O_3) (Ottolini et al. 1993) were used as primary standards to quantify the B content in two samples of norbergite (Norb HV-43 n.4 and Norb HV-47 n.1; Cámara 1997). The quantification was carried out with respect to Si, which was utilized as the internal matrix-element. Average B_2O_3 concentrations and (2σ) relative standard deviations of the Pyrex and NIST glasses are reported in Table 6; the agreement for NIST-610 between the B reference content and that derived from SIMS coincides within the reproducibility of analyses.

The two norbergite samples were then used to derive the $IY(B/Mg)$, which was adopted to quantify the B content in the two crystals of fluoborite. In the sample Fbor HV-43 n.3, SIMS data coincided with the stoichiometric value (18.47 wt% B_2O_3) within the 2σ uncertainty of analysis. On Fbor HV-43 n.2, SIMS yielded a lower value [17.69 ± 0.16 (2σ) wt% B_2O_3] with a relative discrepancy of 3% compared with the other fluoborite (slightly higher than 2σ), and of 4.4% compared with the stoichiometric value. This discrepancy is very low, but it could be related to the different crystallographic orientations. In the case of B in silicates, previous results (Ottolini et al. 1993) provided evidence for low overall matrix effects. These effects are ascribed mainly to the different chemical compositions (in

TABLE 5. Comparison between F data obtained by SIMS and SREF in the studied fluoborite crystals

SAMPLE	matrix	MgO wt%	F wt%	F wt%	rel. st. dev.	d (%)
		ref.	(SREF)	(SIMS)	(2σ %)	
Fbor HV-43 n.3	fluoborite	65.08	24.84	22.06	3.4	11.2
Fbor HV-43 n.2	fluoborite	64.19	24.84	20.67	4.3	16.8

TABLE 6. SIMS data for B in the studied fluoborite crystals and internal standards

SAMPLE	matrix	ref.	ref.	(SIMS)	rel. st. dev.	d (%)
		SiO_2 wt%	B_2O_3 wt%	B_2O_3 wt%	(2σ %)	
Pyrex	glass	80.61	12.86	12.86	3.0	
NIST-610	glass	72.00	0.113	0.122	6.8	7.0
Norb HV-43 n.4	norbergite	29.49		0.183	21	
Norb HV-47 n.1	norbergite	29.72		0.201	14	
		MgO wt%	B_2O_3 wt%	B_2O_3 wt%	(2σ %)	
Fbor HV-43 n.3	fluoborite	65.08	18.47	18.24	1.6	1.0
Fbor HV-43 n.2	fluoborite	64.19	18.47	17.69	1.0	4.4
Norb HV-43 n.4	norbergite	61.11	0.183	0.201	19	9.0
Norb HV-47 n.1	norbergite	60.22	0.201	0.221	15	9.0

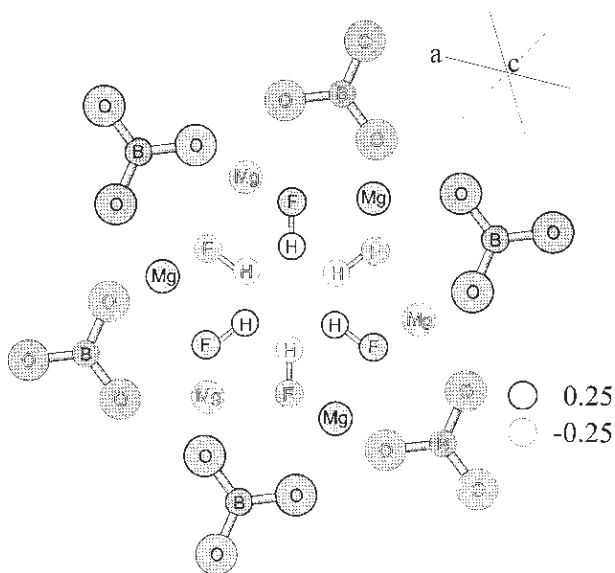
TABLE 7. SIMS data for H in the studied fluorborite crystals and internal standards

SAMPLE	matrix	MgO wt%	H ₂ O* wt%	H ₂ O wt%	rel. st. dev.	d (%)
Fbor HV-43 n.3	fluorborite	ref.	ref.	(SIMS)	(2σ %)	
Fbor HV-43 n.2	fluorborite	65.08	3.40	4.14	4.0	-22
Norb HV-43 n.4	norbergite	64.19	3.59	3.96	5.8	-10
Norb HV-47 n.1	norbergite	61.11	2.21	2.01	2.8	9.0
Norb HV-47 n.7	norbergite	60.22	2.03	2.13	8.2	-5.0
Norb HV-47 n.7	norbergite	60.98	2.27	2.25	7.6	0.9

* Calculated by stoichiometry.

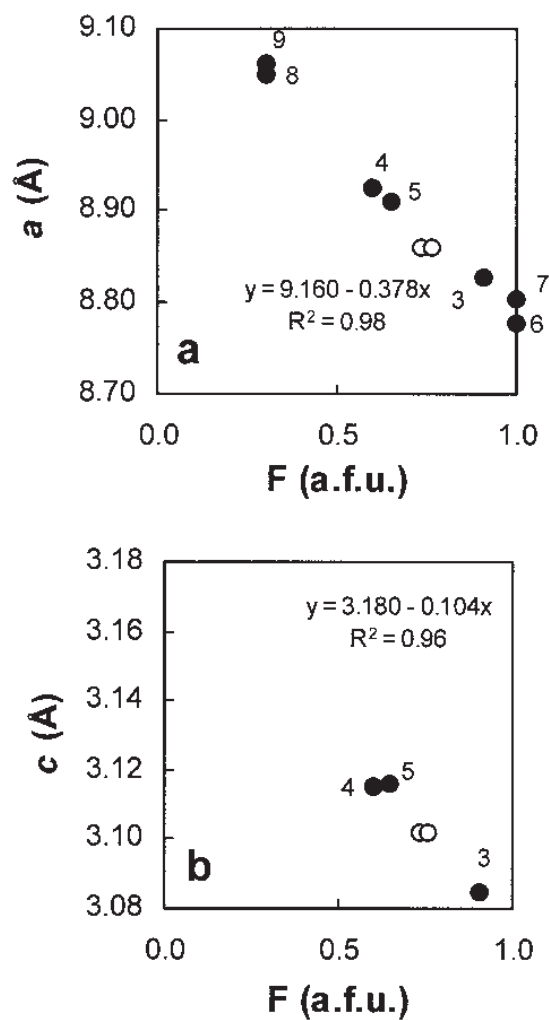
the absence of a controlled sample orientation), typically within ~10% in many silicates. Accuracies on the order of 3% were obtained in many samples (Hawthorne et al. 1995; Ottolini and Hawthorne 1999).

Hydrogen. We followed the procedure described in Ottolini et al. (1995) by using Mg (instead of Si) as the internal reference element for the matrix. As a reference for H₂O content in Mg-rich samples, here represented by fluorborite, we used the stoichiometric values from three norbergites [Norb HV-47 n.7, Norb HV-47 n.1, and Norb HV-43 n.4, as obtained combining SREF, SIMS, and EMP data (see Table 7)]. The IY(H/Mg) was derived by means of a best fit to experimental data from all three samples. The SIMS H₂O data reported in Table 7 represent the average of three analytical sessions. The uncertainty of the procedure was put at <10% relative. The H₂O values in Fbor HV-43 n.3, derived by SIMS, agreed with the stoichiometric value (3.40 wt% H₂O) at ~20% relative, whereas for the other fluorborite sample, the agreement was within 10% (3.96, against 3.59 wt%). In the former case, the discrepancy is higher than analytical uncertainty. Also in this case, there seems to be a small difference between the two samples, possibly related to the orientation of the crystals.

**FIGURE 1.** The structure of fluorborite projected on (001).

DISCUSSION

The local environment of the H atom is shown in Figure 1, which is a projection of the fluorborite structure on (001). The H atom points toward the center of symmetry, which occurs at the center of a columnar cavity surrounded by F and O atoms. The H atoms occur in groups of three at intervals of 0.25 z/c . This environment precludes the emplacement of cations like Li⁺, Na⁺, K⁺, Ca²⁺, Mg²⁺, Sr²⁺, and Ba²⁺ in these channels as proposed by

**FIGURE 2.** Relationship between F atoms per formula unit (afu) and the (a) a axis (Å) and (b) c axis (Å). Open circles = studied samples; 3 = Dal Negro and Tadini (1974); 4 = Segnit and Lancucki (1963); 5, 6 = Brisi and Eitel (1957); 7 = Flamini (1966); 8 = Geijer (1926); 9 = Takeuchi (1950).

Moore and Araki (1976). These cations cannot be present contemporaneously with H due to charge repulsion. Alternatively, their occurrence requires a complicated ordering scheme along the tunnel. The refined site occupancy of the H atom is rather low but it is complementary to that of F and fits well with the SIMS H estimation.

The new data show some geometrical differences from the refinement of Takeuchi (1950) in which the $\langle\text{Mg-O}\rangle$ and $\langle\text{Mg-F}\rangle$ bond lengths are out of the range of normal values, but the obtained results agree well with those of Dal Negro and Tadini (1974). In particular, the individual $\langle\text{B-O}\rangle$ cation-anion distance as of 1.388 Å is nearly equivalent to their value (= 1.381 Å). It also fits well with the $\langle\text{B-O}\rangle$ distance for triangular coordination found in other minerals (1.351–1.403 Å; Hawthorne et al. 1996). $\langle\text{Mg-F}\rangle$ distances reported by Dal Negro and Tadini (1974) are shorter than those found in the present samples in accordance with the higher fluorine content of their crystal. An extrapolation from the values of those authors and from the results obtained here gives an octahedral $\langle\text{Mg-O}\rangle$ of 2.072 Å, slightly shorter than the usual mean bond length for $^{\text{VI}}\text{Mg}$ in silicates (= 2.077 Å). This may be ascribed to the collapse of the structure due to the $\text{OH}_{1/2}\text{F}$ substitution.

SIMS analyses agree well with the EMP analyses and with the stoichiometric values. However, the refined site scattering indicates higher quantities of F than those obtained by SIMS or EMPA. This overestimation of F by SREF can be attributed to local order problems with the position of F and O atoms in the same site (Ottolini et al. 2000).

Hydrogen refined site scattering is slightly lower than that estimated by SIMS in the case of sample Fbor HV-43 n.3. In the other case, the H_2O values coincide within the analytical reproducibility of both techniques. Considering that the H occupancy is <25%, these results indicate how accurate SREF can be for H analysis when good-quality crystals are available and relatively high-resolution data collection is performed.

ESTIMATION OF FLUORINE CONTENT FROM CELL PARAMETERS OF FLUOBORITE

A linear correlation was found between F content and unit-cell parameters, and predictive equations were calculated from data presented here and other published results (Fig. 2). The literature data show more scatter for the c axis but because this axis is very short, the older data probably are affected by bias in powder standard methods of d -spacing determination. If we do not consider the outliers, the calculated equation is c (Å) = $3.180 - 0.104 [\text{F}]$ ($R^2 = 0.96$; 5 points). However, the data for the a axis are much more consistent, giving a (Å) = $9.160 - 0.378 [\text{F}]$ ($R^2 = 0.98$; 9 points). Thus, the cell parameters for a hypothetical OH end-member fluoborite would be $a = 9.16$ Å and $c = 3.18$ Å. This result shows that the structure expands mainly perpendicular to the c axis (3.7 times more than parallel to this axis) as the $\text{OH}_{1/2}\text{F}$ substitution takes place. This difference is due to the presence of H atoms in the hexagonal columns that are coupled with longer HO-M distances. The oxygen atoms separate from the M cation because part of their charge is balanced by the H. No considerations could be made for FeMg_{-1} as Fe^{2+} is only present in trace amounts in the available data.

However, because the structure is F-rich, only a small amount of FeMg_{-1} substitution is expected due to the F-Fe avoidance typically found in minerals.

ACKNOWLEDGMENTS

The authors thank J. Currás (University of Granada, Spain), who kindly provided the samples and S. Bigi (University of Modena, Italy) for assistance with the EMP analyses. The clarity of this manuscript greatly improved after the comments of J.R. Hinthorne and R.J. Tracy. The authors are indebted to D.S. Lauretta (Arizona State University) for helping us to improve the English version of the manuscript. The Consiglio Nazionale delle Ricerche is acknowledged for financing the electron microprobe laboratory in Modena University and the ion microprobe at CSCC (Pavia), whose facilities were used in the present work. Financial support to F.C. is from a FPU research grant of the Spanish M.E.C.

REFERENCES CITED

- Armstrong, J.T. (1988) Quantitative analysis of silicates and oxide minerals: Comparison of Monte-Carlo, ZAF and Phi-Rho-Z procedures, *Microbeam Analysis*, p 239.
- Blessing, R.H., Coppens, P., and Becker, P. (1974) Computer analysis of step scanned X-ray data. *Journal of Applied Crystallography*, 7, 488–492.
- Brisi, C. and Eitel, W. (1957) Identity of nocerite and fluoborite. *American Mineralogist*, 42, 288–293.
- Busing, W.R., Martin, K.O., and Levy, H.A. (1962) ORFLS, a Fortran crystallographic least-squares program. Oak Ridge National Laboratory. Rep. ORNL-TM-305.
- Cámara, F. (1997) New data on the structure of norbergite: hydrogen location by X-ray crystallography. *Canadian Mineralogist*, 35, 1523–1530.
- Dal Negro, A. and Tadini, C. (1974) Refinement of the crystal structure of fluoborite, $\text{Mg}_3(\text{F},\text{OH})_2(\text{BO}_3)$. *Tschermaks mineralogische und petrographische Mitteilungen*, 21, 94–100.
- Flamini, A. (1966) Sulla composizione chimica della nocerite. *Periodico di Mineralogia*, 35, 205–222.
- Geijer, P. (1926) Norbergite and fluoborite, two new minerals from the Norberg mining district. *Geologiska föreningens i Stockholm förhandlingar*, 48, 84.
- Hawthorne, F.C. (1983) Enumeration of polyhedral cluster. *Acta Crystallographica*, A39, 724–736.
- Hawthorne, F.C., Cooper M., Bottazzi P., Ottolini L., Scott Ercit T., and Grew E.S. (1995) Micro-analysis of minerals for boron by SREF, SIMS and EMPA: A comparative study. *Canadian Mineralogist*, 33, 389–397.
- Hawthorne, F.C., Burns, P.C., and Grice, J.D. (1996) The crystal chemistry of boron. Cap. 2 in *Reviews in Mineralogy*, 33, 41–110.
- Lehmann, M.S. and Larsen, F.K. (1974) A method for location of the peaks in step-scan-measured Bragg reflections. *Acta Crystallographica*, A30, 580–584.
- Moore, P.B. and Araki, T. (1974) Pinakiolite, $\text{Mg}_2\text{Mn}^{2+}\text{O}_2[\text{BO}_3]$; warwickite $\text{Mg}(\text{Mg}_{0.5}\text{Ti}_{0.5})\text{O}[\text{BO}_3]$; wightmanite $\text{Mg}_3\text{O}(\text{OH})_2[\text{BO}_3]_n\text{H}_2\text{O}$: crystal chemistry of complex 3 Å wallpaper structures. *American Mineralogist*, 59, 985–1004.
- Moore, P.B. and Araki, T. (1976) Painite, $\text{CaZrB}[\text{Al}_6\text{O}_{18}]$: its crystal structure and relation to jeremjevite, $\text{B}_3[\text{p}_2\text{Al}_6(\text{OH})_2\text{O}_{13}]$, and fluoborite, $\text{B}_3[\text{Mg}_9(\text{F},\text{OH})_2]$. *American Mineralogist*, 61, 88–94.
- North, A.C.T., Phillips, D.C., and Mathews, F.S. (1968) A semi-empirical method of absorption correction. *Acta Crystallographica*, A24, 351–359.
- Ottolini, L. and Hawthorne, F.C. (1999) An investigation of SIMS matrix effects on H, Li and B ionization in tourmaline. *European Journal of Mineralogy*, 11, 679–690.
- Ottolini, L., Bottazzi, P., and Vannucci, R. (1993) Quantification of lithium, beryllium and boron in silicates by Secondary Ion Mass Spectrometry using Conventional Energy Filtering. *Analytical Chemistry*, 65, 1960–1968.
- Ottolini, L., Bottazzi, P., Zanetti, A., and Vannucci, R. (1995) Determination of hydrogen in silicates by Secondary Ion Mass Spectrometry. *Analyst*, 120, 1309–1313.
- Ottolini, L., Cámara, F., and Bigi, S. (2000) An investigation of matrix effects in the analysis of fluorine in humite-group minerals by EMPA, SIMS and SREF. *American Mineralogist*, 85, 89–102.
- Robinson, K., Gibbs, G.V., and Ribbe, P.H. (1971) Quadratic elongation: a quantitative measure of distortion in coordination polyhedra. *Science*, 172, 567–570.
- Segnit, E.R. and Lancucki, C.J. (1963) Fluoborite from Crestmore, California. *American Mineralogist*, 48, 678–683.
- Takeuchi, Y. (1950) The structure of fluoborite. *Acta Crystallographica*, 3, 208–210.
- Ungaretti, L., Lombardo, B., Domeneghetti, C., and Rossi, G. (1983) Crystal-chemical evolution of amphiboles from eclogitised rocks of the Sesia-Lanzo Zone, Italian Western Alps. *Bulletin de Mineralogie*, 106, 645–672.